N and P-type Zwitterion Gated Organic Field Effect Transistors: Supporting Information

Jasleen Kaur[a], Harsimrat Kaur[a], Loren G. Kaake[a*]

[a] Department of Chemistry, Simon Fraser University, 8888 University Drive, Burnaby, BC, V5A 1S6, Canada

* Corresponding author lkaake@sfu.ca

Table of contents

Materials

Poly(methyl methacrylate) (PMMA, M_w = 120,000 Da), lithium perchlorate ($LiClO_4$, 99.99%), and ferrocene (98%) were purchased from Sigma Aldrich. Acetonitrile (≥99.9%) was purchased from VWR International and 2-butanone (99.5%) was obtained from Acros Organics. Indium tin oxide coated glass substrates (ITO, 15 X 15 mm^2, 60 Ω/sq) were purchased from Colorado Concept Coatings LLC. Platinum wire (Pt, 99.99%) was purchased from Sigma Aldrich, Pt gauze (99.9%) and silver wire (Ag, 99.9%) were purchased from Thermo Fisher Scientific.

P3HT OFETs with PMMA dielectric

Organic field effect transistors (OFETs) with a PMMA dielectric were fabricated in a top gate bottom contact configuration using poly(3-hexylthiophene-2,5-diyl) (P3HT) as a semiconducting layer. Device preparation and measurement occurred inside an inert atmosphere glove box. Devices were fabricated on quartz coated glass substrates that were cleaned by sequential ultrasonication for 15 minutes in water, acetone, and methanol followed by drying with nitrogen. Next, substrates were introduced in piranha solution (3:1 H_2SO_4/H_2O_2 v/v) for 20 minutes, rinsed with water, and dried with nitrogen. After that cleaned substrates were treated with 5 mM trichloro(octadecyl)silane (OTS) solution in bicylcohexyl for 30 minutes, rinsed sequentially with toluene and methanol and then annealed at 180 °C for 10 minutes. Following treatment of the surface, substrates were transferred into an inert atmosphere glove box. Source and drain electrodes (5 nm Cr and 60 nm Au) were deposited on top of OTS treated substrates with a shadow mask using a physical vapor deposition (PVD) system contained inside a glove box. Devices had a channel length of 150 µm and a channel width of 3000 µm. A 10 mg/mL solution of P3HT in chlorobenzene was prepared inside a glove box by stirring at 65 °C. The solution was passed through a 0.45 µm polytetrafluoroethylene (PTFE) syringe filter and spin coated onto the substrates at 2000 rpm for

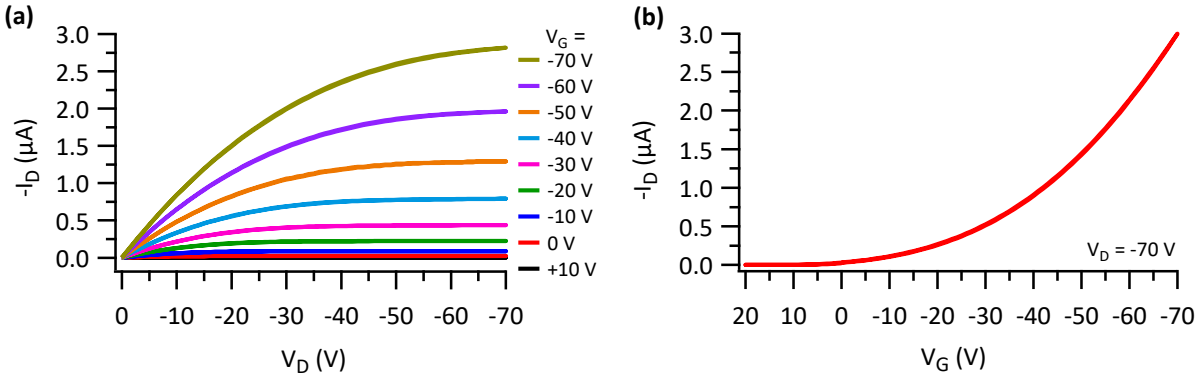

Figure S1. Electrical characteristics under dry conditions for a P3HT OFET using a PMMA dielectric. (a) Output curves for several gate voltages (b) transfer curve at a drain voltage (V_D)= -70 V.

60 s. The obtained P3HT films were approximately 20 nm in thickness, as characterized by a Dektak profilometer. The films were then annealed at 130 °C for 1 hour inside the glovebox. The PMMA dielectric layer was prepared from a 100 mg/mL solution of PMMA in 2-butanone, also prepared inside an inert atmosphere glovebox by stirring the solution at 70 °C. The PMMA solution was filtered through a 0.45 µm PTFE syringe filter and spin coated at 1000 rpm for 60 s over the P3HT layer. Following the spin coating, films were annealed at 105 °C for 5 minutes in the glovebox. The thickness of PMMA film as measured by

a Dektak XT profilometer was 1.4 ± 0.1 µm. A top gate contact (Au, 60 nm) was deposited through a shadow mask using PVD system inside a glovebox.

Output and transfer characteristics were studied inside the glovebox using Keithley 2634B source meter and Keithley 6485 picoammeter at sweep rate of 2 V/s. The representative output and transfer curves are shown in fig. S1a and b. The output curves displayed in fig. S1a show the expected behavior of a carefully prepared P3HT OFET, with clear saturation behavior in the output characteristics and a quadratic dependence on gate voltage (V_G) in the transfer curves (fig. S1b). The output current obtained at V_G = -70 V and drain voltage V_D = -70 V was close to 3 µA in magnitude. The threshold voltage (V_T) and saturated hole mobility (µ) values calculated from the transfer curve shown in fig. S1b are -3.3 V and 0.03 $cm^2V^{-1}s^{-1}$ respectively. A dielectric constant value of 3.0 was used to perform mobility calculations for PMMA device. Notably, the device showed no hysteresis in the transfer curve.

P3HT OFETs with poly(vinyl alcohol) (PVA) dielectric

P3HT OFET devices with PVA dielectric in top gate bottom contact configuration were prepared using the same procedure as described above for the fabrication of P3HT OFETs with PMMA dielectric. After annealing P3HT films inside the glovebox, PVA deposition was carried out under the ambient conditions. PVA solution at a concentration of 100 mg/mL was prepared in water/DMF (1:1 v/v) by stirring at 90 °C for 5 hours. A Zonyl FS 300 fluorosurfactant was added to the PVA solution at concentration of 15 µL/mL. The solution was then filtered through a 0.45 µm PTFE syringe filter and spin coated onto the samples at 1500 rpm for 100 s. The obtained films were then annealed at 100 °C for 20 minutes. The film thickness for PVA determined by Dektak XT profilometer was approximately 0.9 µm. Samples were then transferred to the inert atmosphere glovebox where PVD system is located, and top contact (Au, 60 nm) was deposited through a shadow mask. Measurements of output and transfer curves under dry conditions were done using Keithley 2634B source meter and Keithley 6485 picoammeter at sweep rate of 200 mV/s inside the glovebox. Humidified devices were obtained by humidifying by placing them for 10 minutes in an environmental chamber, where the relative humidity (RH) was fixed at 70%. Devices were removed and their transistor measurements were collected using an Agilent B1500A Semiconductor device

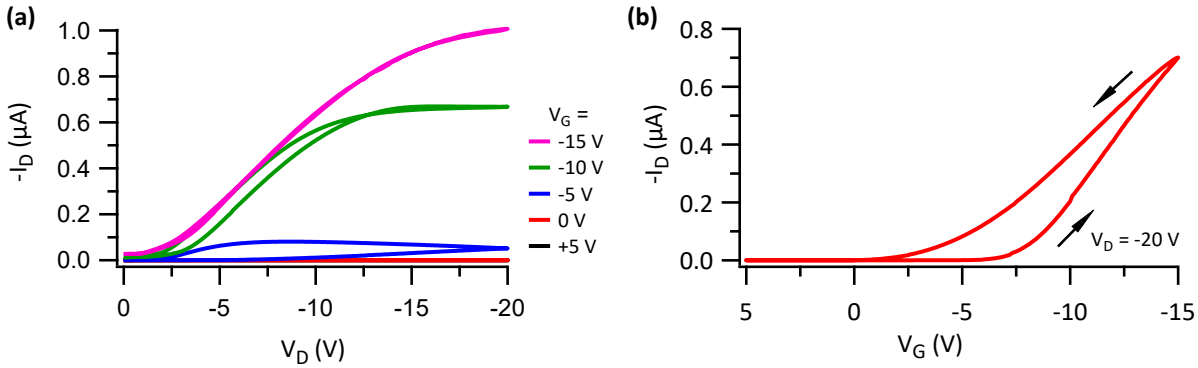

Figure S2. Electrical characteristics under dry conditions for a P3HT OFET with PVA dielectric. (a) Output curves at different gate voltages (b) transfer curve at a drain voltage (V_D) = -20 V.

Analyzer at a sweep rate of 200 mV/s.

Fig S2a and b display representative output and transfer curves for measured P3HT OFET devices using a PVA dielectric material under dry conditions. Threshold voltage and saturated hole mobility values as

calculated from the forward sweep of transfer curve are -6 V and 0.04 $cm^2V^{-1}s^{-1}$, respectively. Hysteresis with a higher back sweep current in the transfer curve is observed. The observation could be related to slow polarization of trace ionic impurities that could be present in PVA.[2] The output and transfer curves

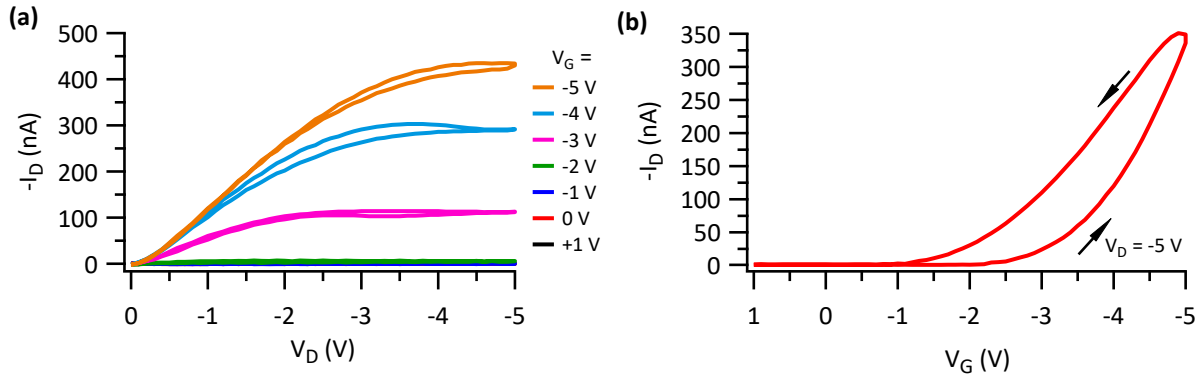

Figure S3. Electrical characteristics of a P3HT OFET with PVA dielectric humidified at RH 70%. (a) Output curves at different gate voltages (b) transfer curve at a drain voltage (V_D) = -5 V.

for P3HT OFET devices using a PVA dielectric material following humidification at RH 70% are shown in fig. S3. The threshold voltage and saturated hole mobility values as calculated from the transfer curves are -2.2 V and 0.02 $cm^2V^{-1}s^{-1}$, respectively. Hysteresis in the transfer curve can be still observed for the humidified device.

Electrochemical doping studies of P3HT

To investigate whether (ZI-PVA) (4-(3-butyl-1-imidazolio)-1-butanesulfonate)-PVA dielectric enable lower voltage operation in OFETs by field effect or electrochemical doping, we studied P3HT films using cyclic voltammetry (CV). We expect that the ions in the electrolyte will intercalate the bulk of P3HT thin films if it is thermodynamically favorable to do so.[3] Electrochemical doping of polymer semiconductors is employed in organic electrochemical transistors (OECT) to achieve high output current for low applied voltages. In this process, mobile ions in the electrolyte migrate under an applied electric field to dope the bulk of polymer semiconductor.[4] As P3HT is a hole conducting polymer, applying negative gate bias in an OECTs results in the diffusion of anions from the electrolyte into the P3HT counterbalancing the charge of induced holes.[3] This phenomenon can be studied in solution with the anion of interest using CV. The appearance of characteristic peaks associated with charging and discharging processes of the semiconductor bulk and large overall currents are indicative of electrochemical doping. In general, migration of zwitterions under an applied field is not feasible due to bound positive and negative charges.[5] We expect that the use of ZI in a CV experiment will result in a smaller overall signal, lacking characteristics typical of bulk doping of P3HT films.

To demonstrate this behavior, we spin coated P3HT film on ITO coated glass, this was used as a working electrode with an active area of 45 mm^2. Prior to spin coating, ITO coated glass substrates were cleaned by sequential ultrasonication in acetone then methanol for 15 minutes and dried with N_2 followed by a plasma treatment for 15 minutes. P3HT solution (10 mg/mL in chlorobenzene) was prepared inside an inert atmosphere glovebox. The obtained solution was filtered through a 0.45 µm PTFE syringe filter. Spin coating took place at 2000 rpm for 60 s, leaving films of approximately 20 nm in thickness as measured by Dektak XT profilometer. Films were annealed at 130 ^oC for one hour inside the glovebox before removing them from the glovebox for the CV measurements. CV measurements were done using CH Instruments Electrochemical Analyzer using Ag wire quasi-reference. The counter electrode was a Pt mesh supported

by a Pt wire. The scan rate was 10 mV/s. Measurements were conducted a 0.1 M solution of ZI prepared in the mixture of acetonitrile/water (99:1 v/v); water in the solvent helped in the complete dissolution of ZI. Solutions were purged with nitrogen for 10 minutes prior to measurement, inert conditions were maintained during the measurement.

Fig. S4a and b shows cyclic voltammograms of P3HT using 0.1 M ZI and 0.1 M $LiClO_4$ solution, respectively. For 0.1 M ZI shown in fig. S4a, an increase in current was observed on scanning to positive potentials with a broader feature on the reverse scan. In comparison to 0.1 M $LiClO_4$ displayed in fig. S4b, the current was lower for ZI, and no peaks were observed. This is consistent with the non-migrating nature of zwitterions under an applied electric field compared to salt solutions/ionic liquids. As an aside, three peaks were seen in oxidative scan (doping) and two for reverse scans (de-doping) in the presence of 0.1 M $LiClO_4$ which is consistent with reported literature. More than one peak in P3HT can arise from the crystalline and

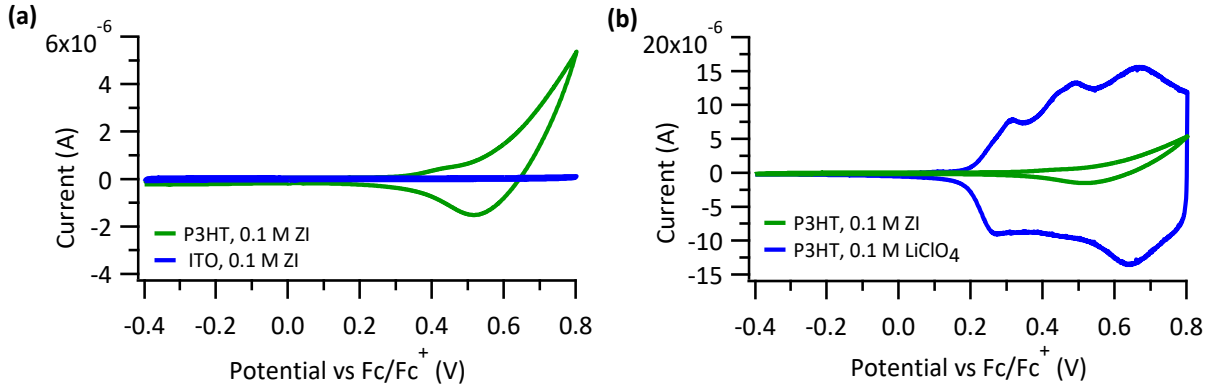

Figure S4. Cyclic voltammograms of P3HT film in 0.1 M ZI and $LiClO_4$ solutions. (a) P3HT films and ITO substrates in 0.1 M ZI in acetonitrile/water (99:1 v/v) solutions. The scan rate was 10 mV/s. (b) P3HT films in 0.1 M ZI compared to 0.1 M $LiClO_4$ in acetonitrile/water (99:1 v/v) solutions. The scan rate was 10 mV/s.

amorphous regions present in P3HT.[6]

Fitting with Havriliak-Negami model

The capacitance versus frequency response of ZI-PVA film was recorded at different relative humidity (RH) values and fitted with Havriliak-Negami equation (eq 1).[7,8] The fits, along with the original data, is shown in fig. S5. The function reproduces the data accurately over the entire frequency range. The values of the parameters used to fit different RH are summarized in table S1. The values of the resistance (R) are provided in somewhat atypical units of Ω cm^2. This can be converted to the device resistance by dividing by the device area (0.385 cm^2). In all cases, the leakage resistance exceeded 10 MΩ. The fitting function also produced fits of adequate quality without this term; it was included to quantify the extent to which the observed low frequency behavior could be explained through a non-zero leakage component. The large resistance obtained from the fits indicates that this contribution is negligible.

$$C(v) = C_\infty + \frac{(C_0 - C_\infty)}{(1 + (i2\pi v\tau)^\beta)^\gamma} + \frac{1}{Rv} \quad (1)$$

Effect of voltage on frequency-dependent capacitance

Capacitance versus frequency response of ZI-PVA film at different applied AC voltages and relative humidities is shown in fig. S6a-d. Metal-insulator-metal capacitors prepared by spin coating ZI-PVA film on gold coated quartz substrates with vapor deposited gold top contact (diameter =1 mm) were measured. At a given RH, increasing voltage leads to a small increase capacitance at lower frequencies (below 100 Hz) except at the lowest humidity (RH 40%). This is consistent with the idea that the zwitterion molecules interact with the PVA in the dielectric material. A large driving voltage can help to disrupt these interactions, allowing a greater percentage of the ZI molecules to align with the field, creating a greater electric field at the metal-dielectric interface. The response time of the devices did not appear to change at lower humidity levels as demonstrated by an unchanged frequency dependent capacitance. At the highest humidity levels, the device response slowed. Given the increase in low frequency capacitance, we interpret this result in terms of a larger RC time constant. The microscopic interpretation of the resistance in this material is challenging, but is likely due to the rotational mobility of the ZI molecules in the highly viscous medium of the hydrated PVA sample.

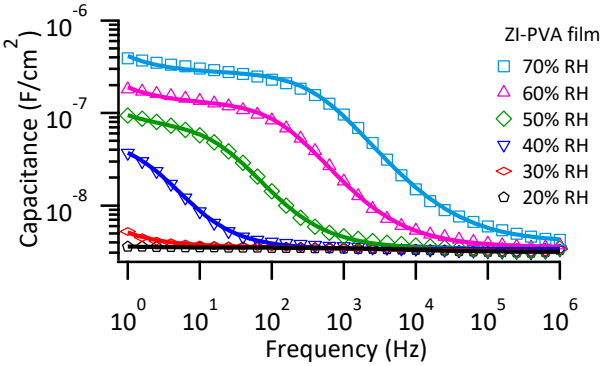

Figure S5. Frequency dependent capacitance response of a ZI-PVA dielectric film. Areal capacitance versus frequency at different RH values and the fit to a Havriliak-Negami function. Data shown with markers and fits with solid lines (reproduced from fig. 3 in the main body of the manuscript).

Table S1. Coefficients used to fit capacitance versus frequency data at different RH.

Parameter	*RH 20%*	*RH 30%*	*RH 40%*	*RH 50%*	*RH 60%*	*RH 70%*
C_∞(nF/cm²)	3.14	2.72	3.37	3.39	3.56	4.03
C_0 (nF/cm²)	3.52	4.26	43.53	74.81	132.25	279.78
τ (s)	2.19×10^{-5}	8.21×10^{-4}	7.16×10^{-2}	6.83×10^{-3}	9.83×10^{-4}	3.10×10^{-4}
β	0.58	0.11	0.84	0.81	0.79	0.77
γ	1.00	1.00	1.00	1.00	1.00	1.00
R (Ω cm²)	1.13×10^{10}	7.11×10^{8}	2.56×10^{8}	4.55×10^{7}	1.71×10^{7}	7.38×10^{6}

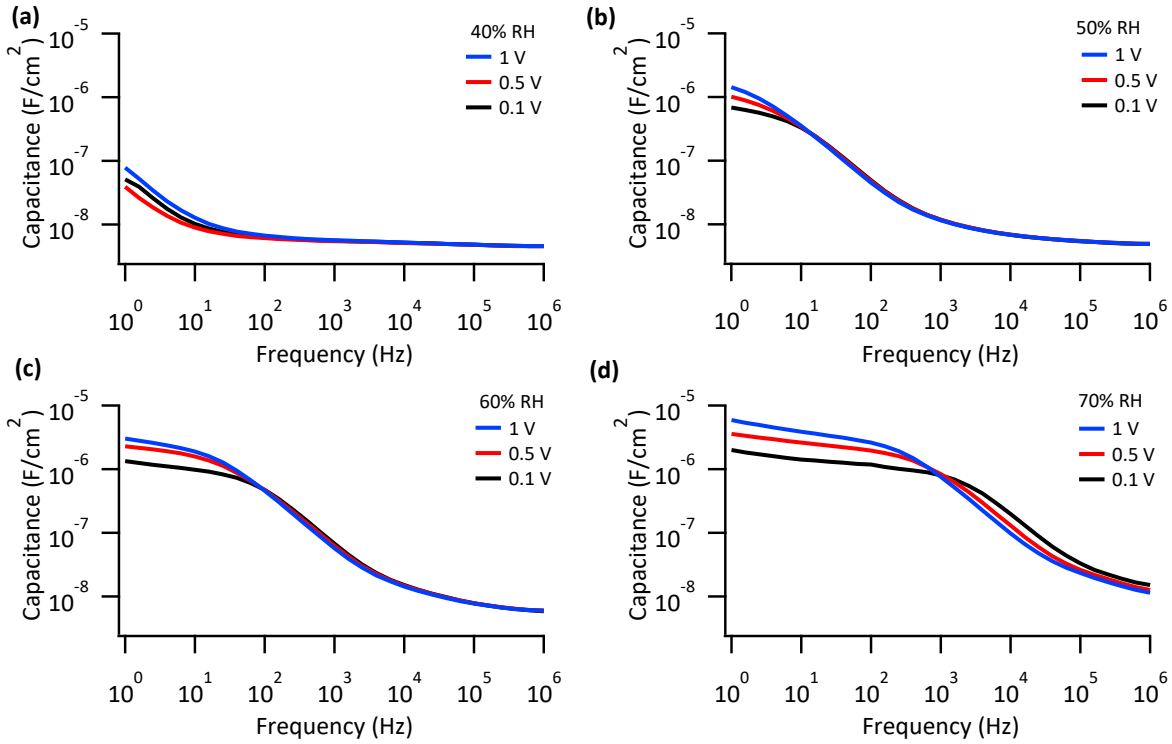

Figure S6. Frequency dependent capacitance response of a ZI-PVA dielectric film at different voltages. (a) Areal capacitance versus frequency at 0.1 V, 0.5 V, and 1 V at 40% RH, (b) 50% RH, (c) 60% RH, and (d) 70% RH.

Impurity capacitance response

In order to quantify the extent to which trace impurities present in the ZI material contributed to the observed capacitance response, impedance measurements were performed on PVA thin films as well as PVA thin films intentionally doped with NaCl, as model for trace ionic impurities in the as-received ZI material. Metal-insulator-metal capacitors were fabricated on 15 x 15 mm titanium substrates cleaned by sequential sonication in acetone, isopropanol, and water. Next, they were placed in 15% HCl solution for 20 minutes and rinsed with water followed by drying with nitrogen. PVA was dissolved in water and dimethyl formamide (DMF) at a mass ratio of 100 mg/ml. The DMF and water were present as a 1:1 (v/v) mixture. Solutions were stirred at 90 ^{o}C for 5 hours with added NaCl at concentration 5 µg/mL. The concentration of NaCl was calculated from information available on maximum ionic impurities which can be present in commercially available ZI used in this study. Samples NaCl-PVA and PVA without NaCl were prepared by spin coating onto the clean titanium substrates at 1500 room for 60 s, followed by annealing at 100 ^{o}C for 20 minutes. Samples were then transferred to an inert atmosphere glovebox where 70 nm of gold was deposited as top contact (diameter = 7 mm) using a shadow mask. Capacitance versus frequency response of films was measured at RH = 50% and results are shown in fig S7. Capacitance remained low and indistinguishable from PVA hinting that impurities are not primarily responsible for the observed capacitance response.

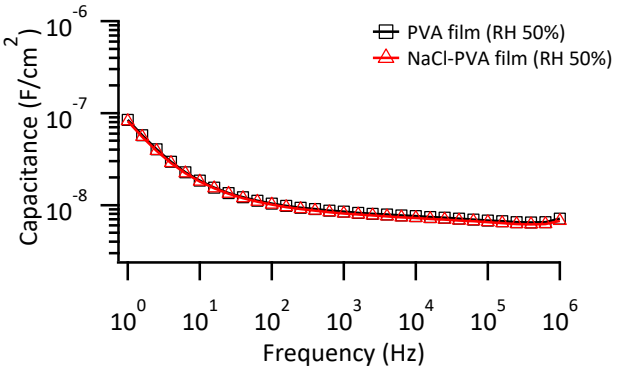

Figure S7. Frequency dependent capacitance response NaCl-PVA and PVA films. Areal capacitance versus frequency of a NaCl-PVA film and a PVA film at RH 50%.

Thermal analysis

Thermogravimetric analysis (TGA) at a heating rate of 5 ^{o}C/min was performed using a PerkinElmer STA 6000 on PVA powder and pure ZI powder samples to identify the decomposition temperature prior to differential scanning calorimetry (DSC) measurements. The results shown in fig. S8a and b indicate that both the PVA and pure ZI powder showed no decomposition ≤ 200 ^{o}C which, therefore, was selected higher temperature limit for running DSC measurements. The measurements also show a slight dip at 100 ^{o}C indicating the presence of a small amount of water. Fig. S8c shows the results of DSC measurements for the second heating and cooling cycle of a ZI-PVA film, a PVA film, and pure ZI powder handled at RH ≤ 30%. The first heating cycle achieved a maximum temperature of 200 ^{o}C, above the temperature where pure ZI powders were observed to melt (fig. 4a). During the cooling cycle, the DSC traces showed no

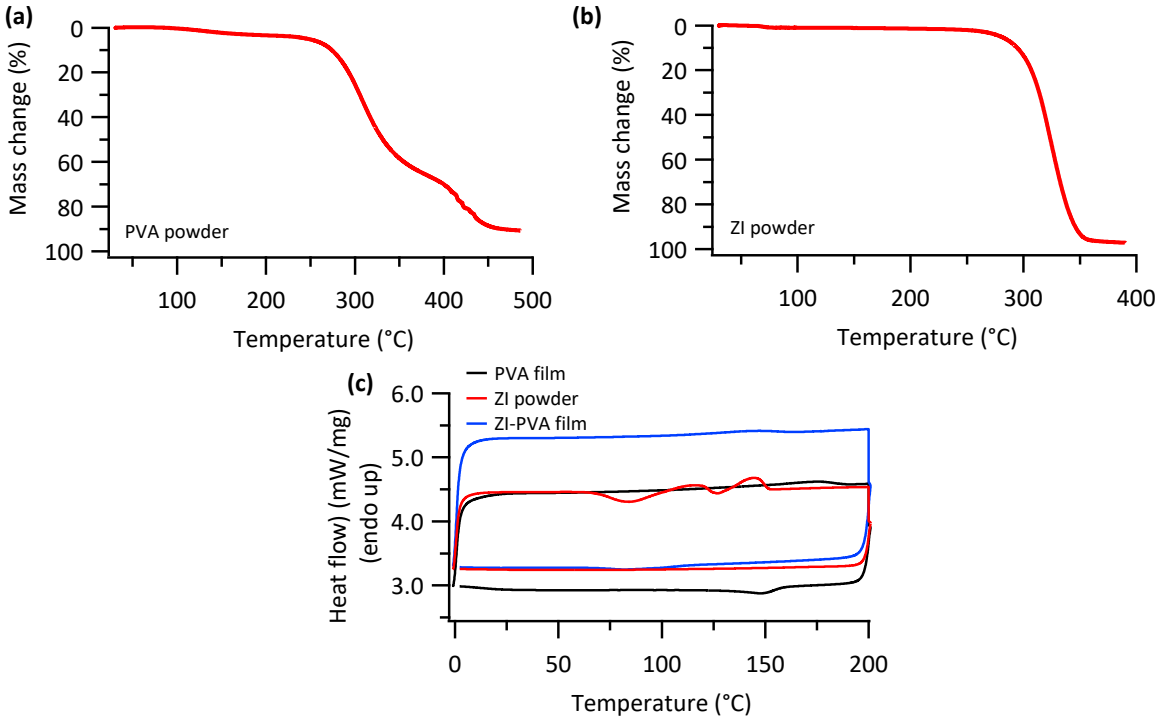

Figure S8. Thermal analysis of ZI, PVA, and ZI-PVA samples. (a) TGA measurement for a PVA powder sample at a scan rate of 5 ^{o}C/min. (b) TGA measurement for pure ZI powder at a scan rate of 5 ^{o}C/min. (c) DSC traces for the second heating and cooling scan at a scan rate of 5 ^{o}C/min for a ZI-PVA film, a PVA film, and a pure ZI powder handled at a RH ≤ 30%.

evidence for the crystallization of the compound, down to the lowest measured temperature at $^{o}0$ C. This indicates that ZI remains a supercooled liquid after melting in the first heating scan. Exothermic crystallization peaks can be seen in the second heating scan (fig. S8c) before the melting peak, which was observed at 144.6 ^{o}C. The features of ZI-PVA film and PVA film were observed to be similar for both first and second DSC heating and cooling cycles. This hints that the phase behavior of ZI is quite rich and warrants further investigation.

References:

1 M. Na and S.-W. Rhee, Electronic characterization of Al/PMMA[poly(methyl methacrylate)]/p-Si and Al/CEP(cyanoethyl pullulan)/p-Si structures, *Org. Electron.*, 2006, **7**, 205–212.

2 M. Egginger, S. Bauer, R. Schwödiauer, H. Neugebauer and N. S. Sariciftci, Current versus gate voltage hysteresis in organic field effect transistors, *Monatsh. Chem.*, 2009, **140**, 735–750.

3 L. G. Kaake, B. D. Paulsen, C. D. Frisbie and X.-Y. Zhu, Mixing at the Charged Interface of a Polymer Semiconductor and a Polyelectrolyte Dielectric, *J. Phys. Chem. Lett.*, 2010, **1**, 862–867.

4 P. Shiri, D. Neusser, C. Malacrida, S. Ludwigs and L. G. Kaake, Mixed Ion-Carrier Diffusion in Poly(3-hexyl thiophene)/Perchlorate Electrochemical Systems, *J. Phys. Chem. C*, 2021, **125**, 536–545.

5 H. Ohno, M. Yoshizawa-Fujita and Y. Kohno, Design and properties of functional zwitterions derived from ionic liquids, *Phys. Chem. Chem. Phys.*, 2018, **20**, 10978–10991.

6 S. Sweetnam, K. R. Graham, G. O. Ngongang Ndjawa, T. Heumüller, J. A. Bartelt, T. M. Burke, W. Li, W. You, A. Amassian and M. D. McGehee, Characterization of the Polymer Energy Landscape in Polymer:Fullerene Bulk Heterojunctions with Pure and Mixed Phases, *J. Am. Chem. Soc.*, 2014, **136**, 14078–14088.

7 J. S. Harrison, D. A. Waldow, P. A. Cox, R. Giridharagopal, M. Adams, V. Richmond, S. Modahl, M. Longstaff, R. Zhuravlev and D. S. Ginger, Noncontact Imaging of Ion Dynamics in Polymer Electrolytes with Time-Resolved Electrostatic Force Microscopy, *ACS Nano*, 2019, **13**, 536–543.

8 A. Schönhals and F. Kremer, in *Broadband Dielectric Spectroscopy*, Springer, Berlin, Heidelberg, 2003, pp. 59–98.